

Water Content and Superconductivity in $\text{Na}_{0.3}\text{CoO}_2 \cdot y\text{H}_2\text{O}$

J. Cmaidalka^a, A. Baikalov^{a,b}, Y. Y. Xue^{a,b}, R. L. Meng^{a,b}
and C. W. Chu^{a,b,c,d}

^aTexas Center for Superconductivity and Advanced Materials, University of
Houston, Houston, Texas 77204-5002, U S A

^bDepartment of Physics, University of Houston, Houston, Texas 77204-5005, U S A

^cLawrence Berkeley National Laboratory, 1 Cyclotron Road, Berkeley, California
94720, U S A

^dHong Kong University of Science and Technology, Hong Kong

Abstract

We report here the correlation between the water content and superconductivity in $\text{Na}_{0.3}\text{CoO}_2 \cdot y\text{H}_2\text{O}$ under the influences of elevated temperature and cold compression. The x-ray diffraction of the sample annealed at elevated temperatures indicates that intergrowths exist in the compound at equilibrium when $0.6 < y < 1.4$. Its low-temperature diamagnetization varies linearly with y , but is insensitive to the intergrowth, indicative of quasi-2D superconductivity. The T_c -onset, especially, shifts only slightly with y . Our data from cold compressed samples, on the other hand, show that the water-loss non-proportionally suppresses the diamagnetization, which is suggestive of weak links.

Key words: water content, sodium cobalt oxyhydrate superconductor,
superconductivity

PACS: 74.70.-b, 74.62.Bf, 74.62.-c

It was recently reported [1] that the layered sodium cobalt oxyhydrate $\text{Na}_x\text{CoO}_2 \cdot y\text{H}_2\text{O}$ ($x = 0.3$, $y = 1.4$) is superconductive with a T_c slightly below 5 K. This compound consists of two-dimensional CoO_2 layers separated by layers of Na^+ and H_2O . The discovery has generated great interest due to the similarity between this cobalt oxyhydrate and cuprates. Unfortunately, our knowledge about the role of the H_2O intercalation in superconductivity is

Corresponding author. Tel.: +1-713-743-8310; fax: +1-713-743-8201; e-mail: yxue@uh.edu

still sparse, although it seems to be one of the dominant factors. The y was estimated by several chemical techniques as between 1.24 and 1.47 for the fully hydrated compound [1]. Slight differences exist between two later neutron diffraction investigations with the lattice water contents being 1.25(2) and 1.48(3), respectively [2,3]. Several non-superconducting phases with similar structures and distinct water contents of $y = 0.6$, 0.3, and 0.1 have also been suggested through thermogravimetric analysis (TGA) investigation [4]. It has been reported that the superconducting phase is extremely chemically unstable. Even exposure for 30 min at 35 °C in dry air may completely kill the superconductivity [4]. It has also been noticed that the room-temperature compression will degrade the superconductivity [1]. All of these degradations were attributed to the loss of water [1,4]. Its exact nature, however, is not well known. Therefore, we measured the y , the superconducting signal size, and the phase composition after the samples were annealed at elevated temperature or cold-compressed. Our data show that: 1) intergrowth superconducting phases exist for $0.6 < y < 1.4$; 2) the zero-field-cooled magnetization, M_{ZFC} , of these intergrowth phases varies linearly with $y - y_0$, while the T_c -onset shifts negligibly, where $y_0 = 0.6$ is the water content of the non-superconducting phase; and 3) the severe suppression of M_{ZFC} by cold compression, however, is associated with a negligible water loss and unchanged x-ray diffraction (XRD) patterns, suggestive of weak-links.

The parent compound $\text{Na}_{0.7}\text{CoO}_2$ and the de-intercalated $\text{Na}_{0.3}\text{CoO}_2$, as well as the superconducting $\text{Na}_{0.3}\text{CoO}_2 \cdot y\text{H}_2\text{O}$ phase, were synthesized following the procedure detailed in Refs. [1,4,5]. No attempt was made to adjust or measure the sodium content, so the reported value of 0.3 is accepted based on the weight ratio of Br: $\text{Na}_{0.7}\text{CoO}_2$ adopted in our Na de-intercalation process. The structures were determined by XRD using a Rigaku DMAX/B III diffractometer. The phase composition was estimated based upon the intensity ratio between the main line of each phase. The microstructure was determined with a JEOL JSM 6400 scanning electron microscope (SEM) operated at 25 kV. The thermogravimetric and differential thermal analysis (TGA/DTA) data were acquired using a TA Instruments SDT 2960 TGA-DTA. The magnetic properties were measured using a Quantum Design SQUID magnetometer.

The XRD patterns are in good agreement with previous publications (Fig. 1). The lines in Fig. 1 from top to bottom correspond to the parent compound $\text{Na}_{0.7}\text{CoO}_2$, the $\text{Na}_{0.3}\text{CoO}_2$ phase immediately after the Br de-intercalation, and the superconducting $\text{Na}_{0.3}\text{CoO}_2 \cdot 1.4\text{H}_2\text{O}$, respectively. All lines of $\text{Na}_{0.3}\text{CoO}_2 \cdot 1.4\text{H}_2\text{O}$ (bottom) above the noise floor can be indexed based on the $P6_3/mmc$ crystalline group, demonstrating that the samples are single-phase structurally. The SEM images of a $\text{Na}_{0.7}\text{CoO}_2$ sample and a $\text{Na}_{0.3}\text{CoO}_2 \cdot 1.4\text{H}_2\text{O}$ sample display hexagonal plate-like grains, suggesting well-crystallized grains with sizes of $1\text{--}20\text{ }\mu\text{m}$ in the a ; b direction (Figs. 2a,b). Irregular interlayer micro-cleavages, however, appear much more frequently in the water-intercalated

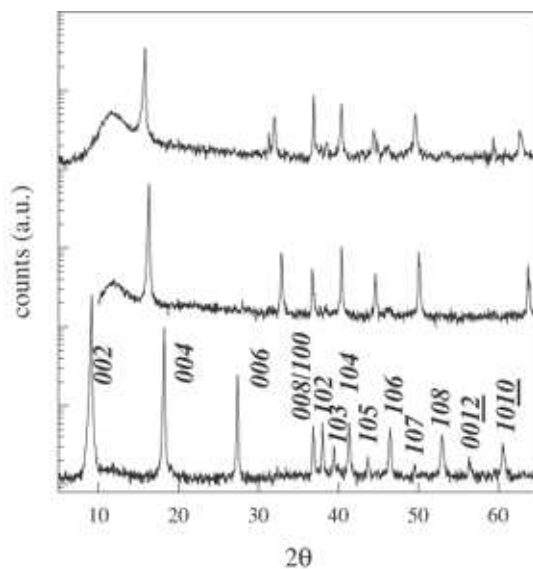


Fig. 1. XRD patterns of $\text{Na}_{0.7}\text{CoO}_2$ (top); $\text{Na}_{0.3}\text{CoO}_2$ (middle); and $\text{Na}_{0.3}\text{CoO}_2 \cdot 1.4\text{H}_2\text{O}$ (bottom).

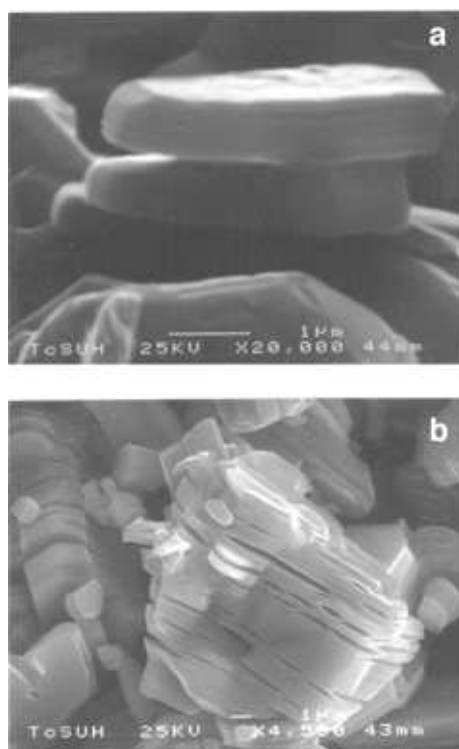


Fig. 2. SEM images of (a) $\text{Na}_{0.7}\text{CoO}_2$ and (b) $\text{Na}_{0.3}\text{CoO}_2 \cdot 1.4\text{H}_2\text{O}$.

samples.

The TGA-DTA was used to estimate the H_2O content under various conditions. A $\text{Na}_{0.3}\text{CoO}_2$ powder sample was measured between 25 and 600 °C with a fast sweep rate of 20 °C/min (Fig. 3). The apparent water

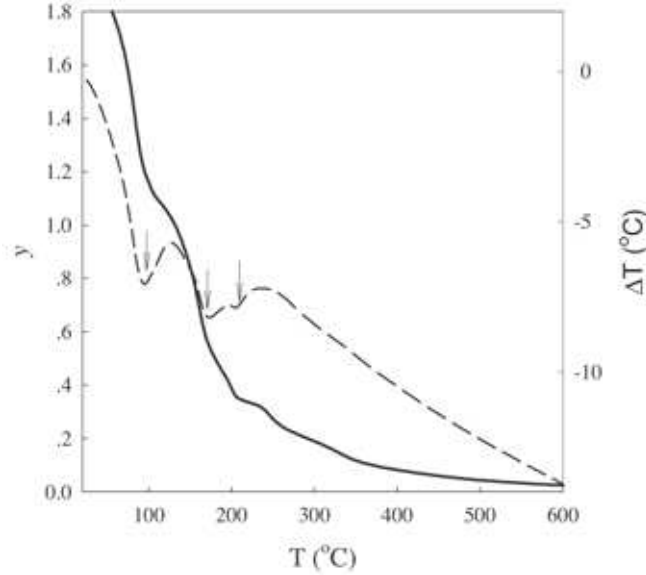


Fig. 3. TGA (solid line) and DTA (dashed line) of a fully hydrated $\text{Na}_{0.3}\text{CoO}_2 \cdot y\text{H}_2\text{O}$ sample with sweep rate of $20^\circ\text{C}/\text{min}$. The arrows show endothermic peaks.

content, y , was estimated based on the remaining weight above 600°C , where $\text{Na}_{0.3}\text{CoO}_{2-z}$ is assumed to be the stable phase, where z represents the possible oxygen deficiency at elevated temperatures [2]. A $z = 0.2$ is used here to match the reported $y = 1.4$ at the fully hydrated state at slower sweep rate (see below). Three endothermic peaks can be clearly seen in the DTA trace above 50°C with corresponding plateaus in the TGA data. Despite the non-equilibrium nature of this fast run, which causes uncertainty in the values of y and T associated with the DTA peaks, the endothermic peaks demonstrate the existence of partially dehydrated phases, as reported previously [2].

To further explore the equilibrium condition of $\text{Na}_{0.3}\text{CoO}_2 \cdot y\text{H}_2\text{O}$, TGA was measured again with a slower sweep rate of $0.25^\circ\text{C}/\text{min}$ in under flowing oxygen (solid line in Fig. 4). It is interesting to note that there is a small kink around 25°C with the corresponding $y = 1.4$. When TGA is done in the static room air (i.e. 61% relative moisture at 21°C), the 25°C kink develops into a plateau and shifts slightly to $30\{34^\circ\text{C}$ due to the slower dehydration rate, but the corresponding y value remains unchanged (dashed line in Fig. 4). This is in rough agreement with the reported equilibrium condition of 23°C and 40% relative moisture [2]. The total water content, on the other hand, varies from sample to sample. The "extra" water above the plateau, therefore, should be attributed to the surface water absorbed. The heating procedure, therefore, is used to measure the crystalline water. The y values of 0.7 and 0.1 at the respective 60°C and 150°C plateaus are also in rough agreement with the previous results [4]. The fully hydrated compound, therefore, is stable only within a rather narrow temperature-moisture range without extra surface water.

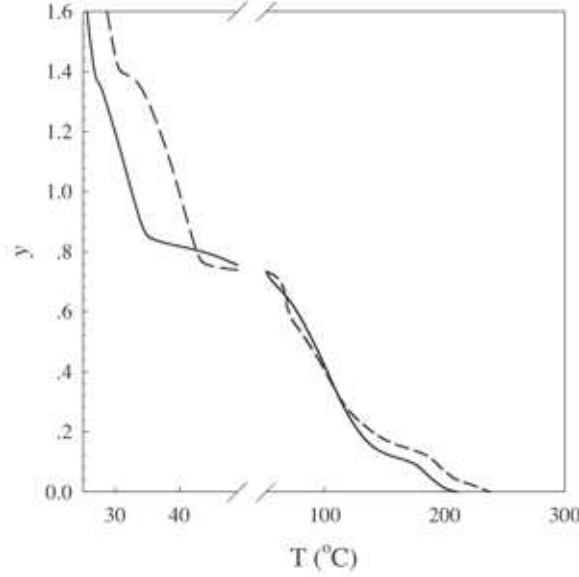


Fig. 4. TGA of $\text{Na}_{0.3}\text{CoO}_2 \cdot y\text{H}_2\text{O}$ with a sweep rate of $0.25^\circ\text{C}/\text{m}$ in under flowing oxygen (solid line) and under static room air (dashed line) of 61% relative moisture at 21°C .

Whether the phases with $0.6 < y < 1.4$ are stable and how they behave remain unknown. Jorgesen et al. suggested that the $\text{Na}_x\text{CoO}_2 \cdot y\text{H}_2\text{O}$ should be a distinct phase with $x = 1/3$ and $y = 4x$ based on the structure observed [2]. The deviations from the predicted $1/3$ and $4/3$, in such a model, should not only affect the superconductivity, but the microstructure as well. The equilibrium vapor pressure reported, on the other hand, shows a noticeable change when y varies from 1.0 to 0.6 [2], a phenomenon not exactly consistent with the miscibility gap expected between two distinct equilibrium phases, but suggestive of the possible intermediate states. To explore this issue, TGA was acquired as a function of time at 40°C in air (Fig. 5). The y value dropped from $y_1 = 1.4$ to $y_0 = 0.7$ in 30 min, which is in rough agreement with the results of Foo et al. The XRD and superconductivity were then measured at both the fully hydrated state and after a 40°C , 15 min annealing in room air, where a $y = 0.9$ is expected (the arrow in Fig. 5). The XRD pattern of the annealed sample reveals, however, a major phase of $\text{Na}_{0.3}\text{CoO}_2 \cdot 0.6\text{H}_2\text{O}$ with 10% $\text{Na}_{0.3}\text{CoO}_2 \cdot 1.4\text{H}_2\text{O}$ (dashed bars with indices underlined, Fig. 6), whose 002 line can barely be noticed. The (002) lines of the $\text{Na}_{0.3}\text{CoO}_2 \cdot 0.6\text{H}_2\text{O}$ (solid bars with indices, Fig. 6), on the other hand, are highly distorted and asymmetric. A broad shoulder on its left side spreads continuously to the (002) line of $\text{Na}_{0.3}\text{CoO}_2 \cdot 1.4\text{H}_2\text{O}$. This feature is inconsistent with that caused by typical microstrain and small grain size on the one hand, and differs from that of amorphous phases on the other hand. Intergrowth between $\text{Na}_{0.3}\text{CoO}_2 \cdot 1.4\text{H}_2\text{O}$ and $\text{Na}_{0.3}\text{CoO}_2 \cdot 0.6\text{H}_2\text{O}$, therefore, is proposed, although the detailed structure analysis is beyond our scope. The conjecture is supported by the fact that the (004) lines of the two phases are symmetric, well separated, and relatively narrow. The (100) line, especially, is as sharp as that in Fig. 1,

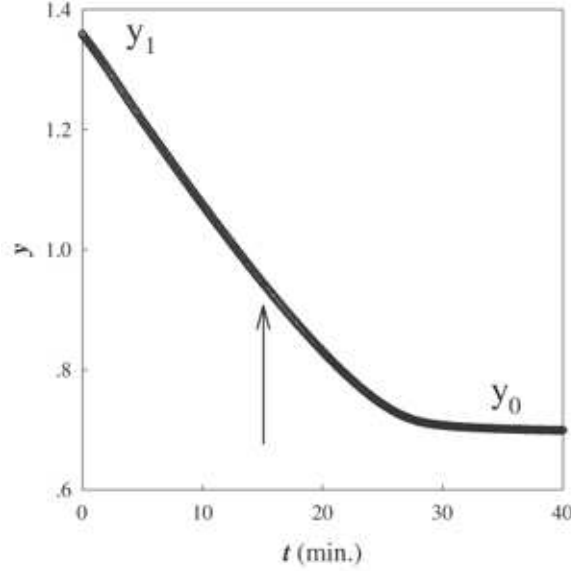


Fig. 5. Isothermal TGA curve of a $\text{Na}_{0.3}\text{CoO}_2 - y\text{H}_2\text{O}$ sample at 40°C .

suggesting a rather long in-plane coherence length, i.e. 100 nm or longer. The randomly distributed water vacancies should affect the (100) and (001) lines in similar ways. This is in agreement with the general consideration of the lattice-distortion energy in intercalated systems. It should also be pointed out that the average "extra" water $y = 0.23$ from the TGA trace is far greater than the possible water content of the residual $\text{Na}_{0.3}\text{CoO}_2 - 1.4\text{H}_2\text{O}$ ($= 0.1$). Most of the "extra" water has to exist in the intergrowth phases. As a result, a large part of the CoO_2 layers may possess interlayer environments different from that of $\text{Na}_{0.3}\text{CoO}_2 - 1.4\text{H}_2\text{O}$. To verify whether these intermediate intergrowth phases are thermodynamically stable at a fixed y , 100 mg of annealed sample was sealed in a 0.5 cc plastic container. No noticeable changes in the XRD pattern were observed after a 12 hr, 40°C annealing. It should be noted that the TGA data in Fig. 5 suggest the water-loss (intake) rate is relatively fast, with a time-scale of 10 min. These data, therefore, suggest that the intergrowth phases are stable, when the water content is fixed, and that the water stoichiometry may be realized through intergrowth.

The zero-field-cooled magnetization, M_{ZFC} , was then measured to explore the effects on superconductivity (Fig. 7). The 15 min, 40°C annealing suppresses $|M_{\text{ZFC}}|$ by 3.7 and 2.5 times at 2 and 3 K, respectively. $y = y_0$, on the other hand, decreases 2.9 times. The $|M_{\text{ZFC}}|$ suppression is far smaller than the value expected, i.e. > 10 , if only $\text{Na}_{0.3}\text{CoO}_2 - 1.4\text{H}_2\text{O}$ is superconducting. Most intergrowth phases, therefore, may be superconducting as well, although the non-equilibrium nature of $|M_{\text{ZFC}}|$ prohibits a quantitative comparison. It is also interesting to note that the T_c onset has not been shifted within our experimental resolution of 0.1 K (Inset, Fig. 7). The suppression of $|M_{\text{ZFC}}|$, in fact, is smaller when the temperature approaches T_c . The diamagnetic signal seems to be roughly proportional to $y - y_0$ with no indication of T_c -degradation with

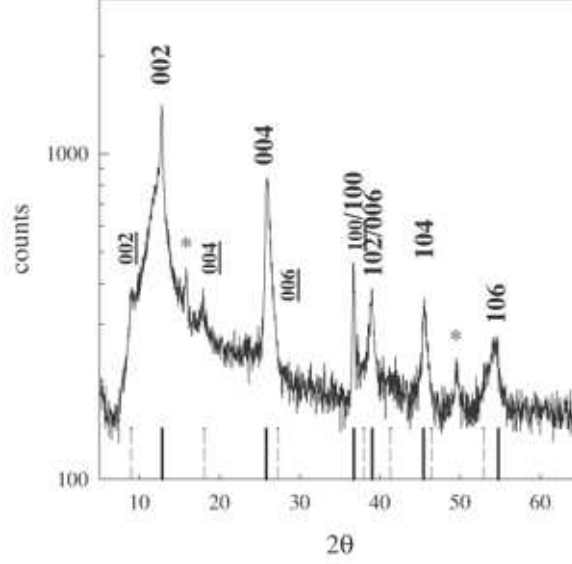


Fig. 6. The XRD of a $\text{Na}_{0.3}\text{CoO}_2 \cdot 1.4\text{H}_2\text{O}$ sample after annealing for 15 min at 40°C : * $\{\text{Na}_{0.3}\text{CoO}_2\}$; solid bars with indices $\{\text{Na}_{0.3}\text{CoO}_2 \cdot 0.6\text{H}_2\text{O}\}$; and dashed bars with indices underlined $\{\text{Na}_{0.3}\text{CoO}_2 \cdot 1.4\text{H}_2\text{O}\}$.

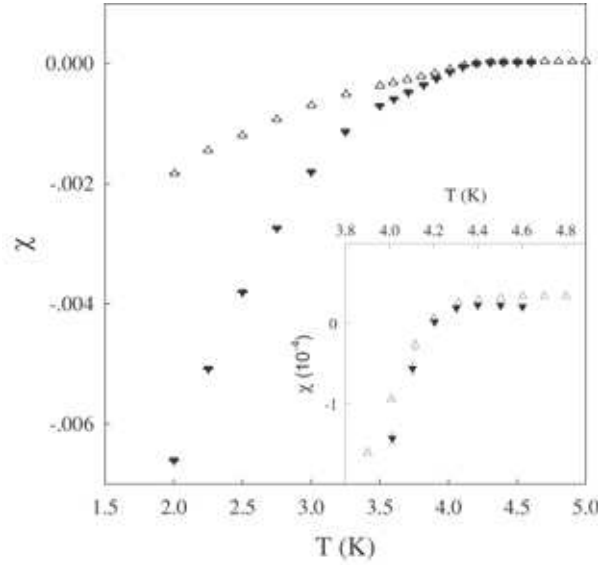


Fig. 7. The zero-field-cooled susceptibility: χ ($\text{Na}_{0.3}\text{CoO}_2 \cdot 1.4\text{H}_2\text{O}$; Δ) after 15 min, 40°C annealing in air. Inset: for an expanded T -scale near the T_c -onset.

intergrowth. The data, therefore, suggest a quasi-2D superconductivity. The CoO_2 - CoO_2 layer separation, $\sim 1\text{ nm}$, is comparable with the c -axis coherence length. Those intergrowth phases with a few sequential (0.3Na) - $0.7\text{H}_2\text{O}$ - CoO_2 - $0.7\text{H}_2\text{O}$ - (0.3Na) blocks, therefore, may possess the same superconductivity as that of the fully hydrated $\text{Na}_{0.3}\text{CoO}_2 \cdot 1.4\text{H}_2\text{O}$.

We have also compressed several pellets at ambient temperature using a standard die-and-piston set (10 mm diameter). Significant suppression of M_{ZFC}

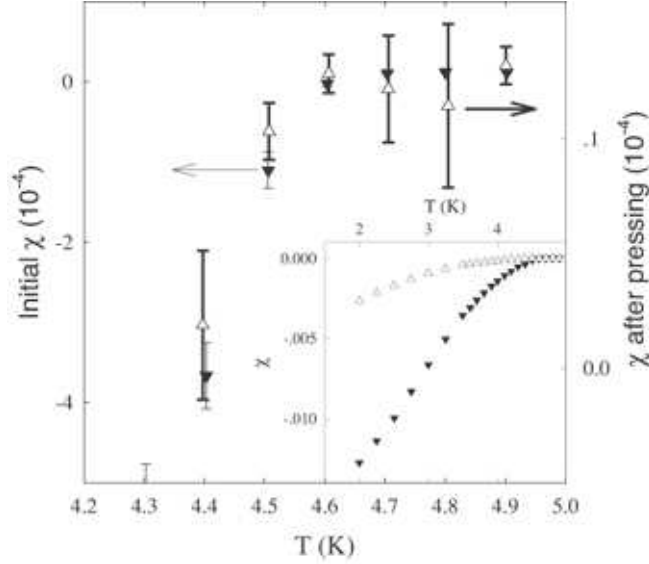


Fig. 8. The onset after compression. Note the different scales used. Inset: $\chi(T)$. Δ : the initial $\text{Na}_{0.3}\text{CoO}_2 \cdot 1.4\text{H}_2\text{O}$ powder; \blacktriangle : after 11000 lb cold-compression.

is observed in all cases. A typical case with a load equal to 11000 lb is shown in the inset of Fig. 8. The $\chi_{\text{ZFC}} = M_{\text{ZFC}}/H$ at 2 K and 5 Oe is suppressed from the initial value ($0.17 = 4\mu$) to $0.03 = 4\mu$ by the cold compression. However, the weight loss due to compression is mainly the surface water and the crystalline water loss is rather small (Fig. 9). The χ at the 25 °C plateau decreases by less than 0.05 after the compression. This value is far from enough to cause the four-fold suppression of M_{ZFC} if the M_{ZFC}/χ still holds. Additionally, there are no noticeable impurity phases in the XRD pattern, excluding the possibility of significant pressure-induced decomposition (Fig. 10). The line widths, which were suggested to be characteristic of "poor" superconductors [4], are the same as those of the "good" samples of Ref. [4]. In fact, the full-width at half height of the first three (001) lines are close to our instrument resolution even after the cold compression. It should also be pointed out that the T_c -onset shift is relatively small, 0.1 K in this particular case, although shifts as large as 0.4 K have also been observed (Fig. 8). All of these observations demonstrate that the T_c suppression under cold compression cannot be understood in terms of crystalline-water loss or pressure-induced decomposition alone. Weak links associated with the pressure-induced lattice defects, such as cracks and dislocations in grains, may be a reasonable interpretation.

In summary, we have studied the effects of water content and cold compression on the superconductivity of the newly discovered superconductor $\text{Na}_{0.3}\text{CoO}_2 \cdot 1.4\text{H}_2\text{O}$. While the compound is chemically unstable, the water-loss through slow annealing leads to intermediate intergrowth phases. The superconducting signal size is determined by the average water content, and is insensitive to the intergrowth. On the other hand, the severe M_{ZFC} degradation after cold compression is accompanied only by negligible crystalline-water

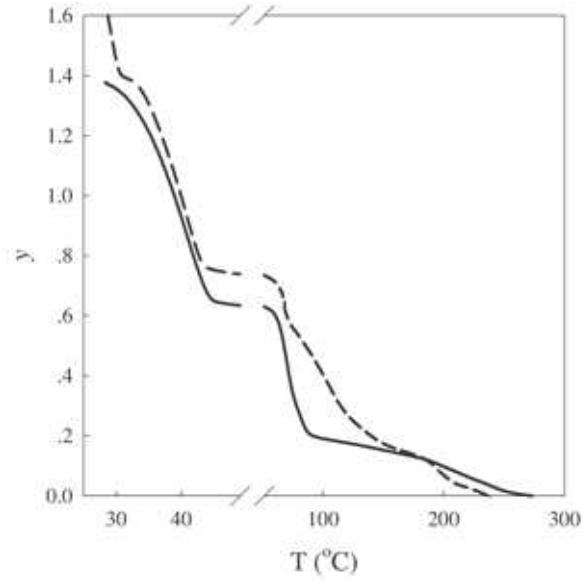


Fig. 9. TGA curves of the cold-compressed sample $\text{Na}_{0.3}\text{CoO}_2 \cdot y\text{H}_2\text{O}$ (solid line) and the initial powder sample of $\text{Na}_{0.3}\text{CoO}_2 \cdot y\text{H}_2\text{O}$ (dashed line).

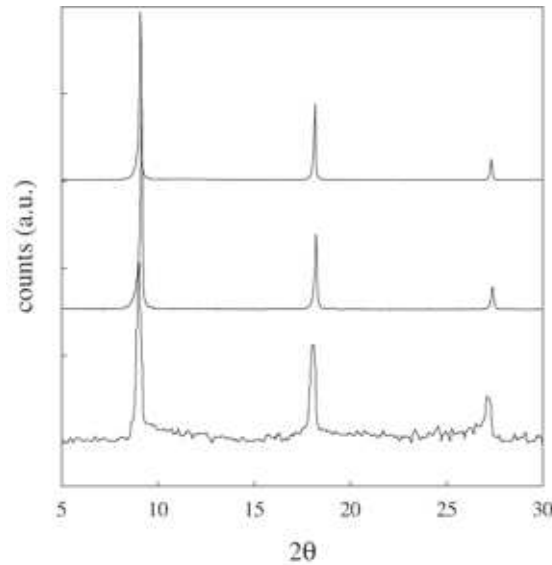


Fig. 10. The XRD from top to bottom : the initial sample; the cold-compressed sample; the "good" superconducting powder data taken from Ref. [4].

loss. The creation of weak links, therefore, is proposed to be the cause.

Acknowledgements

The authors would like to thank Y. Y. Sun for x-ray analysis. This work is supported in part by NSF Grant No. DMR-9804325, the T. L. L. Temple

Foundation, the John J. and Rebecca Moores Endowment, and the State of Texas through the Texas Center for Superconductivity and Advanced Materials at the University of Houston; and at Lawrence Berkeley Laboratory by the Director, Office of Basic Energy Sciences, Division of Materials Sciences and Engineering of the U.S. Department of Energy under Contract No. DE-AC03-76SF00098.

References

- [1] K. Takada, H. Sakurai, E. Takayama-Muromachi, F. Izumi, R. A. Dilanian and T. Sasaki, *Nature* 422, 53 (2003).
- [2] J. D. Jorgensen, M. Avdeev, D. G. Hinks, J. C. Burley and S. Short, *cond-mat/0307627* (2003).
- [3] J. W. Lynn, Q. Huang, C. M. Brown, V. L. Miller, M. L. Foo, R. E. Schaak, C. Y. Jones, E. A. Mackey and R. J. Cava, *cond-mat/0307263* (2003).
- [4] M. L. Foo, R. E. Schaak, V. L. Miller, T. Klimczuk, N. S. Rogado, Y. Wang, G. C. Lau, C. C. Haley, H. W. Zandbergen, N. P. Ong and R. J. Cava, *cond-mat/0304464* (2003).
- [5] R. E. Schaak, T. Klimczuk, M. L. Foo and R. J. Cava, *cond-mat/0305450* (2003).